

Hailong Shang<sup>a,b</sup>, Bingyang Ma<sup>a</sup>, Rongbin Li<sup>b</sup>, Geyang Li<sup>a</sup>

<sup>a</sup>State Key Laboratory of Metal Matrix Composites, Shanghai Jiao Tong University, Shanghai, P.R. China

<sup>b</sup>School of Mechanical Engineering, Shanghai Dianji University, Shanghai, P.R. China

## Formation of intermetallic compounds and their effect on mechanical properties of aluminum–titanium alloy films

Al–Ti alloy films with various Ti contents were prepared through magnetron co-sputtering with Al and Ti targets and treated with vacuum annealing at 400 °C. Energy dispersive spectroscopy, X-ray diffraction, transmission electron microscopy, X-ray photoelectron spectroscopy and nanoindentation were used to determine the composition, microstructure and hardness of the films to reveal the existence of intermetallic compounds and their effects on the microstructure and mechanical properties. The results showed that Al–Ti films with lower Ti contents formed nanocrystalline structures of highly supersaturated solid solution. With the increase of Ti content, various types of Al–Ti intermetallic compound bonds formed. The existence and increasing concentration of these compound bonds gradually transformed the films into amorphous structures and supported the continual increase of the film hardness, reaching a high value of 8.8 GPa at 36.3 at.% Ti.

**Keywords:** Highly supersaturated solid solution; Intermetallic compound bond; Al-based alloy film; Mechanical properties

### 1. Introduction

Alloy films prepared by physical vapor deposition (PVD) exhibit features of highly supersaturated solid solution (i.e., solute content significantly higher than that of the equilibrium solid solubility). This type of structure remark-

ably improves film performance [1, 2]. For instance, existing studies [3–8] have demonstrated that, when some sputtered Al alloy films form highly supersaturated solid solution, their hardness can reach up to about 8 GPa, equivalent to the hardness level of high-speed steel. This technique therefore became an important approach to produce films with desired properties. However, controversy still exists regarding the underlying driver of the hardness enhancement, especially when the solute content far exceeds its equilibrium solubility limit: whether it is due to structure changes (e.g., highly supersaturated solid solution, or nanocrystal/amorphous structure) or the formation of intermetallic compounds. Some researches believe that in the systems of sputtered Al-based films (e.g., Al–Cr [3], Al–Mo [4], Al–W [5], Al–Mg [9]), when the solute content is much greater than the solid solute limit and even the films possess an amorphous structure, no intermetallic compounds would form. Some researches found that in Al–Cu [7, 8, 10] and Al–Fe [6, 11] alloy films, intermetallic compounds formed at alloy contents great than 1.8 at.% Cu or 50 at.% Fe, respectively. In the case of Al–Ti films however, two different views exist. One maintains that intermetallic compounds cannot form in these films [3, 6, 9] while the other believes it is possible [12]. These different reports on the existence of the intermetallic compounds demonstrate that there is currently no consensus regarding the underlying cause of the alloy hardness enhancement.

This paper reveals conditions and causes of the formation of intermetallic compound bonds in alloy films, through in-

vestigation of microstructures and mechanical properties of Al–Ti sputtered alloy films with different Ti contents.

## 2. Experimental procedure

All the films were synthesized using a multi-target magnetron sputtering system. Pure Al (99.99%) and pure Ti (99.99%) targets, 76 mm in diameter and 5 mm thick, were controlled by DC and RF cathodes, respectively. Stainless steel substrates were polished with 1  $\mu\text{m}$  diamond paste, then ultrasonically cleaned in acetone and alcohol, before being mounted on a substrate holder in the vacuum chamber. The distance between the substrates and the cathodes was about 50 mm. With the base pressure less than  $5 \times 10^{-4}$  Pa, high-purity Ar (99.999%) was introduced into the chamber with a pressure of  $6 \times 10^{-1}$  Pa. After determining the deposition rate of Al target and Ti target at different power levels, a series of 2- $\mu\text{m}$ -thick films with different Ti contents were synthesized by changing the power of the Ti target while holding the power of the Al target constant. No bias voltage or heating was applied to the substrates during the process.

An OXFORD INCA energy dispersive X-ray spectroscopy (EDS) was used to analyze the composition of the films. The phase composition and microstructures of the films were characterized with a Rigaku D/max-2550/PC X-ray diffractometer (XRD), a JEM-2100F transmission electron microscope (TEM) and an AXIS Ultra X-ray photoelectron spectroscopy (XPS). A Fisher scope H100VP nanoindenter with a Vickers indenter was used to measure the hardness of the films. 10 mN of the maximum penetration load was selected. The loading and holding time were both 30 s. The hardness result of each sample was the average value of more than 20 indentations.

## 3. Results

Figure 1 shows the XRD patterns of Al–Ti alloy films with different Ti contents. From the figure, three main Al diffraction peaks  $(111)_{\text{Al}}$ ,  $(200)_{\text{Al}}$  and  $(220)_{\text{Al}}$  are observed in the films with the Ti content of 1.2 at.% and 11.4 at.%, levels well above the solid solution limit ( $<0.1$  at.% Ti). This demonstrates that the films are a single-phase Al solid solution without pronounced preferential orientation. As the Ti content increases, only the  $(111)_{\text{Al}}$  peak remains and the peak diffuses gradually. According to the change of diffraction peak full width at half maximum (FWHM) using the Scherrer formula to calculate the grain size changes with Ti content, Fig. 2 shows that the grain sizes of the films gradually reduced from about 80 nm containing 1.2 at.% Ti to less than 10 nm containing 29.3 at.% Ti. When the Ti content reaches 36.3 at.%, only a very broad diffraction peak exists, indicating an amorphous structure in the film. It is worth noting that the position of the diffraction peak no longer remains at the  $(111)_{\text{Al}}$  position, but shifts towards larger angles slightly.

At the low Ti content level (11.4 and 22.2 at.%), the bright field TEM images shown in Fig. 3a and b show that the grain sizes of the films are about 30 nm and 15 nm respectively, consistent with the results shown in Fig. 2. The selected area electron diffraction (SAED) patterns at the upper left corner exhibit only a set of Al fcc diffraction

rings without any rings or spots of Ti or Al–Ti compounds, indicating the films remain as a single-phase Al solid solution despite Ti content being much higher than the equilibrium solid solubility. The image of the film with 36.3 at.% Ti in Fig. 3c exhibits an amorphous structure and the SAED ring highly diffusive.

In order to investigate whether films with various Ti contents, especially amorphous films, contained intermetallic compounds, the films with 11.4, 22.2 and 36.3 at.% Ti were vacuum annealed at 400  $^{\circ}\text{C}$  for 2 h. Figure 4 shows their as-deposited and annealed XRD patterns. After annealing, the Al diffraction peak of the film with 11.4 at.% Ti strengthens and shifts slightly to the right and a  $(111)_{\text{Al}_3\text{Ti}}$  peak emerges further to the right side. For the film with 22.2 at.% Ti, the diffraction peak at  $(111)_{\text{Al}}$  position obviously moves to the position of the  $(111)_{\text{Al}_3\text{Ti}}$  peak at a larger angle. Meanwhile, several weak  $\text{Al}_5\text{Ti}_2$  diffraction peaks emerge. The results indicate that the as-deposited films with less than 22.2 at.% Ti are metastable highly super-saturated Al solid solution. The dissolved Ti atoms precipitate out and form compounds such as  $\text{Al}_3\text{Ti}$  and  $\text{Al}_5\text{Ti}_2$  after annealing. When

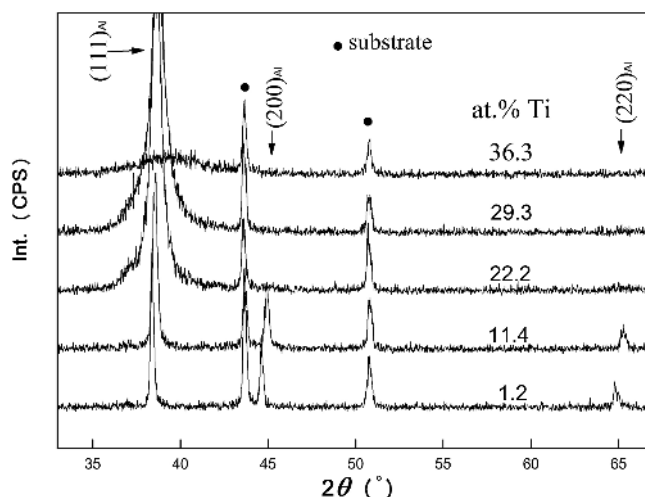


Fig. 1. XRD patterns of Al–Ti alloy films with different Ti contents (● for substrate diffraction peaks).

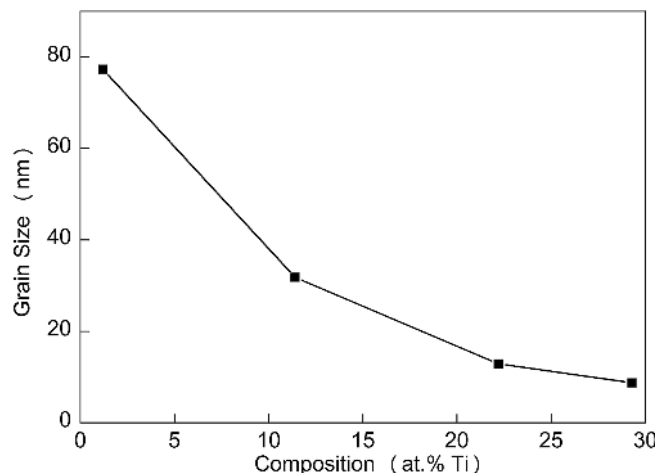


Fig. 2. Change in grain size with Ti content according to XRD and Scherrer formula.

the Ti content reaches 36.3 at.% however, the very broad diffraction peak of the film locates at the original position and remains diffuse after annealing, indicating that the Al atoms of the film exist in the form of various Al–Ti compound bonds even before annealing. High melting temperatures of these compounds make the film difficult to crystallize at 400 °C. In fact, some researches on Al–Ti alloy films have already raised the possibility that improvement in hardness is driven by the formation of Al–Ti compound in the amorphous structures of the films [12]. Unfortunately, no experimental evidence has been presented.

X-ray photoelectron spectroscopy (XPS) was used to further characterize the form of Al present in as-deposited amorphous film containing 36.3 at.% Ti. Figure 5 shows only one Al 2p peak located at 71.7 eV except for the Al–O peak (74.9 eV) from Al<sub>2</sub>O<sub>3</sub> on the sample surface. This peak, away from 72.9 eV of Al–Al, is the superposition of several Al–Ti compound peaks (they are all in the range of 71.4–72.1 eV). This direct characterization result further demonstrates the amorphous film contains various Al–Ti intermetallic compound bonds.

It may be further inferred that although the films with lower Ti content (<22.2 at.%) appear as a highly super-saturated solid solution, Al–Ti compound bonds should exist but have not formed crystals large enough to be detected by XRD or TEM.

Figure 6 shows the relationship between microhardness and Ti content of Al–Ti films. The microhardness of the films rises almost linearly with increasing Ti content, from 2.4 GPa at 1.2 at.% Ti to 8.8 GPa at the 36.3 at.% Ti, with no obvious relationship to microstructure change including nano-crystallization and amorphization.

#### 4. Discussion

The Al–Ti film’s microstructural evolution with increasing Ti content can be attributed to both kinetics and thermodynamics.

In terms of kinetics, the rate by which the sputtered particles lose their high kinetic energy when deposited on the growing surface of films is comparable to an extremely high cooling rate (about 10<sup>13</sup> K s<sup>-1</sup>) for the material [13].

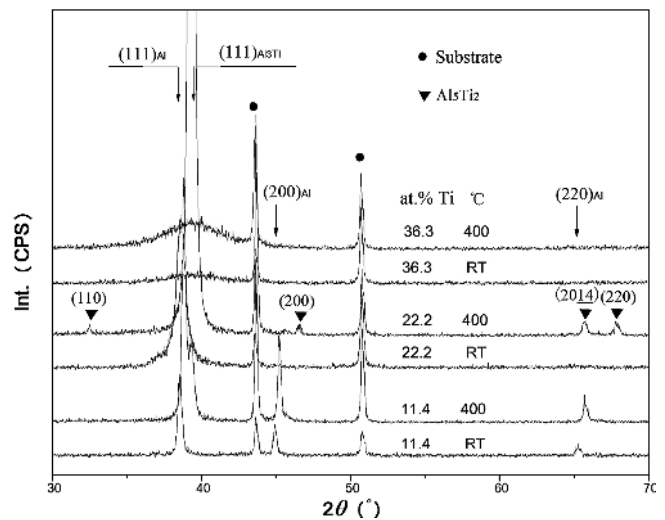


Fig. 4. XRD patterns of the as-deposited films and annealed films with different Ti contents (● for substrate and ▼ for Al<sub>5</sub>Ti<sub>2</sub> diffraction peaks).

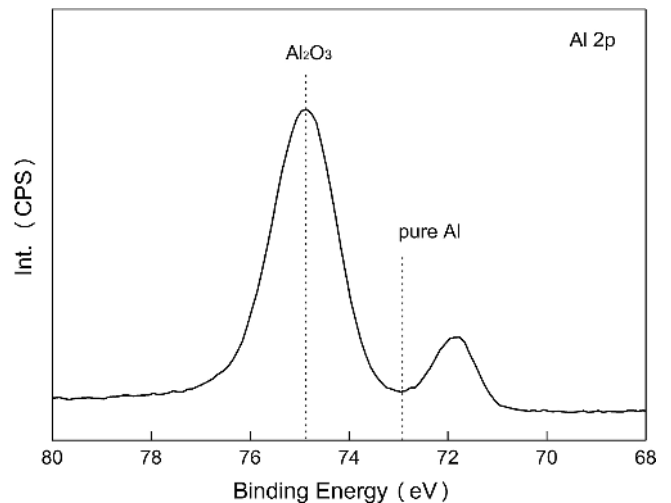


Fig. 5. The XPS Al 2p spectrum of the as-deposited amorphous film containing 36.3 at.% Ti.

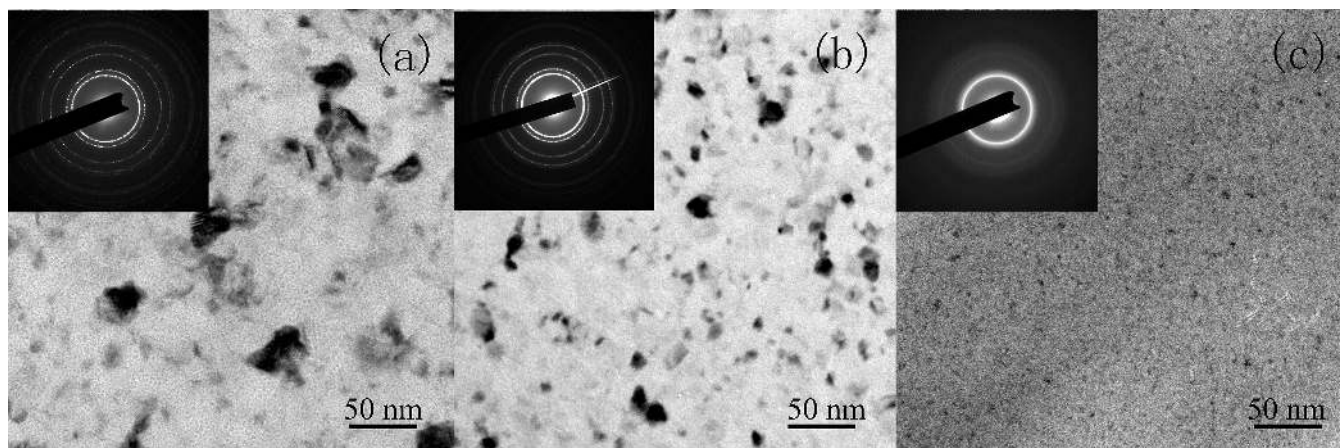


Fig. 3. TEM bright field images and SAED patterns of Al–Ti alloy films with different Ti contents: (a) 11.4 at.% Ti; (b) 22.2 at.% Ti; (c) 36.3 at.% Ti.

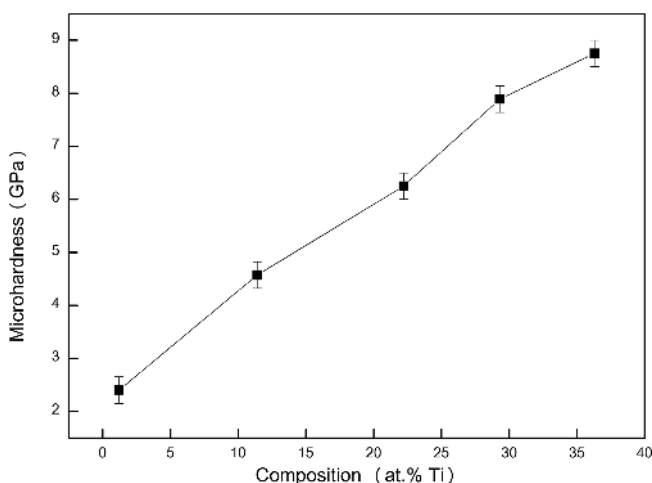


Fig. 6. Hardness variation of alloy films versus Ti concentration.

In this process, sputtered Al particles (atoms, ions or clusters) aggregate and form nanometer-scale grains through short distance migration due to their huge concentration, while the accumulation of Ti particles requires long-range diffusion and overcoming energy barriers [14, 15] due to their low concentration. Given kinetic limitations, Ti atoms tend to stay in the Al lattice, highly supersaturated. The resulting severe lattice distortion even leads to amorphous structures [16].

In terms of thermodynamics, with the increase in Ti content, the ratio of Al/Ti can reach the stoichiometric ratio of various Al–Ti intermetallic compounds such as  $\text{Al}_3\text{Ti}$ ,  $\text{Al}_5\text{Ti}_2$ ,  $\text{Al}_5\text{Ti}_3$ . On the other hand, the impact of high energy sputtered particles on the growing surface in the deposition process facilitates overcoming energy barriers and forming Al–Ti compound bonds. In addition, the random distribution of Ti particles on the growing surface allows compound bonds with different stoichiometric ratios to form. The existence and increasing concentration of these compound bonds gradually transformed the films into amorphous structures.

The hardness increase of the films as Ti content rises is also evidence of the existence of intermetallic compound bonds. Although the increase of the films' hardness can be attributed to solution strengthening [17, 18] and fine grain strengthening [19, 20] at lower Ti content, the continual increase in hardness even when the film becomes amorphous, cannot be explained by the reasoning above, but should be attributed to the effect of the intermetallic compound bonds.

Many published works [3–9] have mostly relied on XRD and SAED to investigate highly supersaturated solid solution of Al alloy films. Because no obvious compound diffraction information was found in Al–Cr [3], Al–Mo [4], Al–W [5], Al–Mg [9] films, their conclusion only focused on solute content and microstructure, but not intermetallic compounds.

Unlike the above alloy systems with many intermetallic compounds at lower content, the Al–Cu system only has one intermetallic compound ( $\text{CuAl}_2$ ) at 0–33 at.% Cu. Additionally, Cu atoms supersaturated dissolved in Al have strong diffusion ability, indicated by its age-hardening temperature below 180 °C. Therefore,  $\text{CuAl}_2$  in

Al–Cu films is easy to enlarge and be detected through XRD or SAED.

Based on the above experimental results and analysis, we believe that all Al matrix binary alloy (they all contain intermetallic compounds) sputtered films contain compound bonds when they exist in the form of amorphous structures or even highly supersaturated solid solutions. The existence and increasing concentration of these compound bonds support the continual increase of hardness of the films.

## 5. Conclusion

Al–Ti alloy films with Ti contents of 1.2–36.3 at.% were prepared and investigated. The results revealed that the films with lower Ti contents formed nanocrystalline structures of highly supersaturated solid solution. With the increase of Ti content, various types of Al–Ti intermetallic compound bonds formed. The existence and increasing concentration of these compounds gradually transformed the films into amorphous structures and supported the continual increase of hardness of the films, reaching a maximum value of 8.8 GPa at 36.3 at.% Ti.

This work was supported by National Natural Science Foundation of China (No. 51371118, No. 51401120 and No. 51671125) and Natural Science Foundation of Shanghai (No. 16ZR1412800).

## References

- [1] E. Botcharova, M. Heilmaier, J. Freudenberger, G. Drew, D. Kudashov, U. Martin, L. Schultz: *J. Alloys Compd.* 351 (2003) 119. DOI:10.1016/S0925-8388(02)01025-3
- [2] T. Tsuda, C.L. Hussey, G.R. Stafford, O. Kongstein: *J. Electrochem. Soc.* 151 (2004) C379. DOI:10.1149/1.1704611
- [3] F. Sanchette, H.L. Tran, A. Billard, C. Frantz: *Surf. Coat. Technol.* 74–75 (1995) 903. DOI:10.1016/0257-8972(94)08210-3
- [4] Z. Lee, C. Ophus, L.M. Fischer, N.F. Nelson, K.L. Westra, S. Evoy, V. Radmilovic, U. Dahmen, D. Mitlin: *Nanotechnology* 17 (2006) 3063. DOI:10.1088/0957-4484/17/12/042
- [5] M. Stubicar, A. Tonejc, N. Radic: *Vacuum* 61 (2001) 309. DOI:10.1016/S0042-207X(01)00135-X
- [6] F. Sanchette, A. Billard: *Surf. Coat. Technol.* 142 (2001) 218. DOI:10.1016/S0257-8972(01)01197-5
- [7] N. Boukhris, S. Lallouche, M.Y. Debilia, M. Draïssia: *Eur. Phys. J. Appl. Phys.* 45 (2009) 30501. DOI:10.1051/epjap/2009016
- [8] M. Draïssia, H. Boudemagh, M.Y. Debili: *Phys. Scr.* 69 (2004) 348. DOI:10.1238/Physica.Regular.069a00348
- [9] A. Perez, F. Sanchette, A. Billard, C. Rébéré, C. Berziou, S. Touzain, J. Creus: *Mater. Chem. Phys.* 132 (2012) 154. DOI:10.1016/j.matchemphys.2011.11.013
- [10] M. Draïssia, M.Y. Debili: *Philos. Mag. Lett.* 85 (2005) 439. DOI:10.1080/09500830500256629
- [11] M.Y. Debili, T.H. Loi, C. Frantz: *Rev. Metall./Cah. Inf. Tech.* 95 (1998) 1501.
- [12] M. Naka, T. Shibayanagi, M. Maeda, S. Zhao, H. Mori: *Vacuum* 59 (2000) 252. DOI:10.1016/S0042-207X(00)00277-3
- [13] P.K. Almqvist, M.A. Ejsing, J. Bøttiger, J. Chevallier: *J. Mater. Res.* 22 (2007) 1018. DOI:10.1557/jmr.2007.0121
- [14] M. Silva, C. Wille, U. Klement, P. Choi, T. Al-Kassab: *Mater. Sci. Eng. A* 445 (2007) 31. DOI:10.1016/j.msea.2006.07.069
- [15] F. Liu: *Appl. Phys. A* 81 (2005) 1095. DOI:10.1007/s00339-004-2965-7
- [16] H.L. Shang, W.Q. Liu, Y.J. Dong, A.M. Zhang, B.Y. Ma, G.Y. Li: *Acta Metall. Sin.* 50 (2014) 395. DOI:10.3724/SP.J.1037.2013.00447
- [17] V. Yamakov, D. Wolf, S.R. Phillpot, A.K. Mukherjee, H. Gleiter: *Nat. Mater.* 1 (2002) 45. DOI:10.1038/nmat700

- [18] G.P.M. Leyson, W.A. Curtin, J.L.G. Hector, C.F. Woodward: Nat. Mater. 9 (2010) 750. DOI:10.1038/nmat2813  
[19] M. Legros, D.S. Gianola, K.J. Hemker: Acta Mater. 56 (2008) 3380. DOI:10.1016/j.actamat.2008.03.032  
[20] T.J. Rupert, D.S. Gianola, Y. Gan, K.J. Hemker: Science 326 (2009) 1686. DOI:10.1126/science.1178226

(Received September 21, 2016; accepted January 9, 2017; online since February 2, 2017)

**Correspondence address**

Prof. Geyang Li  
State Key Laboratory of Metal Matrix Composites  
Shanghai Jiao Tong University  
No. 800, Dongchuan Road  
Shanghai 200240  
P. R. China  
Tel.: +86-13916295066  
Fax: +86-21-37202749  
E-mail: gyli@sjtu.edu.cn

**Bibliography**

DOI 10.3139/146.111480  
Int. J. Mater. Res. (formerly Z. Metallkd.)  
108 (2017) 4; page 257–261  
© Carl Hanser Verlag GmbH & Co. KG  
ISSN 1862-5282